

# A Two-Atom Picture of Coherent Atom-Molecule Quantum Beats

Bogdan Borca<sup>†</sup>, D. Blume<sup>‡</sup>, Chris H. Greene<sup>†</sup>

<sup>†</sup> JILA and Department of Physics, University of Colorado, Boulder, Colorado 80309-0440

<sup>‡</sup> Department of Physics, Washington State University, Pullman, Washington 99164-2814

**Abstract.** A simple two-atom model is shown to describe a Bose-Einstein condensate of alkali atoms subjected to external magnetic field ramps near a Feshbach resonance. The implications uncovered for two atoms in a trap can be applied at least approximately to a many-atom condensate. A connection to observations is accomplished by scaling the trap frequency to achieve a density comparable to that of the experiments, which yields the fraction of atom pairs in the gas that become molecules. A sudden approximation is used to model the external magnetic field ramps in the vicinity of a two-body Feshbach resonance. The results of this model are compared with recent experimental observations of Donley *et al.* [1].

PACS numbers: 03.75.Mn

Submitted to: *New J. Phys.*

## 1. Introduction

Utilizing Feshbach resonance physics, recent experiments have produced an atomic Bose-Einstein condensate (BEC) coherently coupled to molecules in high vibrationally excited bound states [1]. The coupling of atomic and molecular states was achieved through application of a pulsed external magnetic field and it has sparked much interest [2] since it ultimately (although possibly not yet) should lead to the creation of a molecular condensate. The problem of creating a molecular BEC has been one of the focus areas of ultracold physics research for several years now [3]. Two different techniques, namely photoassociation and a magnetic field ramp near a Feshbach resonance, have been used in attempts to transform an atomic condensate into a molecular one. The use of Feshbach resonances to control the atom-atom scattering length, and other properties, has been previously demonstrated experimentally [4, 5].

It was predicted theoretically [6] that magnetic field pulses would drive a significant part of an atomic BEC into a molecular one. These predictions were based on a mean field theory approach, of the same type that has proven very successful in describing most properties of the alkali atom BECs produced experimentally to date. However, two sets of experiments performed at JILA have shown puzzling results that did not match the original theoretical predictions. In one experiment, a single magnetic pulse close to the Feshbach resonance probed the strongly interacting atomic dynamics, [7] while in a second experiment double pulses generated interference patterns between the different states populated. In both experiments, the atoms, part of the initial BEC cloud, were observed to end up in one of the following three components: a remnant BEC cloud, a burst of hot atoms, and a missing (undetected) component. This outcome differed from the theoretical predictions which only accounted directly for two components. The questions regarding the nature of the three components observed experimentally, including the specific issue of whether a molecular BEC was created, were addressed by two independent theoretical papers [8, 9]. Both of these papers accounted for many body effects by employing field theory beyond the mean field (i.e., Gross-Pitaevskii equation) level. These two studies gave similar answers, in identifying the observed atom bursts as hot, non-condensed atoms, and the missing component as a molecular condensate. In addition to the successful theoretical models,[8, 9] three other many-body approaches have also addressed the interpretation of the Donley *et al.* experiment [10, 11, 12].

In this paper we propose an alternative model that does not rely on field theory. Our model considers only two-body dynamics and uses a very simple scaling procedure to apply our results to the many-body system studied experimentally. The observed oscillatory behavior can then be viewed as a simple example of quantum beats of the type that arise whenever indistinguishable quantum mechanical pathways associated with two or more impulsively-excited stationary states interfere coherently.[13] Specifically, our treatment considers two atoms confined by a spherically symmetric harmonic oscillator potential, which interact through a contact potential. The stationary states of such a system have been described by Busch *et al.*, [14] who proposed it as a model that can be

used in the context of ultracold collisions occurring in trapped gases. The properties of this treatment were further investigated in the context of the condensed Bose gases by Julienne and coworkers [15, 16] and by Blume and Greene [17]. These papers investigated the strong interactions that occur near a Feshbach resonance, and employed an energy-dependent scattering length to model this situation. Here we implement this model for a time-dependent magnetic field, with augmented by the sudden approximation to model the rapid field ramps.

By performing a frequency rescaling, an initial condensate density can be achieved for two bodies that is comparable to the density range studied experimentally. The premise of our model is that the energy scale of the trap energy levels is very low in present day experiments, far smaller than the molecular binding energies of interest. At the same time, we anticipate that the physics of any single molecule formation is controlled by the interaction of just two atoms, even in a many-atom condensate. Accordingly, we consider just two atoms in an oscillator trap of very high frequency, adjusted so that the density of the two atoms becomes comparable to the condensate density in the experiments. The resulting two-body approach is then used to model the recent experimental results of Donley *et al.*[1] Our two-body model is shown to describe a number of the nontrivial features observed in the experiment, although discrepancies remain, which may indicate that an inclusion of some many-body effects may be necessary to achieve a full quantitative description. Nevertheless, our results show that more of the key physics has an intrinsic two-body origin than appears to have been realized in existing theoretical models.

This paper is organized as follows: Section 2 determines the eigenstates of two trapped atoms using a quantum-defect-style method that differs from the treatment of Ref. [14] but is equivalent. Section 3 discusses the behavior of the atom pair close to a Feshbach resonance, and our approximate solution of the time-dependent equation using the sudden approximation. Section 4 discusses the frequency rescaling employed to interpret the many-atom system. Section 5 compares the results of our model with recent experiments, while Section 6 summarizes our conclusions.

## 2. Two Interacting Atoms in a Trap

We consider two atoms of mass  $m$  in a spherical oscillator trap of angular frequency  $\omega$ , which interact through a zero-range potential  $V(\mathbf{r})$ ,

$$V(\mathbf{r}) = \frac{4\pi\hbar^2 a_{\text{sc}}}{m} \delta^{(3)}(\mathbf{r}) \frac{\partial}{\partial r} r. \quad (1)$$

Here  $a_{\text{sc}}$  is the two-body atom-atom scattering length and  $\mathbf{r}$  is the relative coordinate of the two particles. The Hamiltonian of the two-body system separates into a center of mass part and a relative part. The center of mass part has the usual harmonic oscillator solutions which are not affected by the scattering length; hence, we focus on the relative motion in the following.

Since the contact potential in Eq. (1) acts solely on the  $s$ -wave symmetry, we consider only solutions of the relative Schrödinger equation with zero orbital angular momentum. We define the harmonic oscillator length  $a_{\text{ho}} = \sqrt{\hbar/(\omega m/2)}$  corresponding to the *reduced* mass,  $m/2$ , as our length scale, leading to a dimensionless radial coordinate  $x = r/a_{\text{ho}}$ . Our energy unit is chosen to be  $\hbar\omega$ , resulting in a dimensionless energy variable  $\epsilon = E/\hbar\omega$ . The  $s$ -wave eigenfunction  $\phi_{\epsilon,l=0}$  of the radial Schrödinger equation in the relative coordinate corresponding to energy  $\epsilon\hbar\omega$  is then rescaled,

$$\phi_{\epsilon,l=0} = \frac{u(x)}{x} \frac{1}{\sqrt{4\pi}}, \quad (2)$$

so that the radial equation has only second derivatives,

$$\left( -\frac{1}{2} \frac{d^2}{dx^2} + \frac{1}{2}x^2 \right) u(x) = \epsilon u(x). \quad (3)$$

The contact potential, Eq. (1), imposes a boundary condition on the logarithmic derivative of  $u(x)$  at the origin:

$$\frac{u'(0)}{u(0)} = -\frac{a_{\text{ho}}}{a_{\text{sc}}}. \quad (4)$$

Solutions of these equations have been obtained by Busch *et al.* [14]. However, we now rederive these solutions in a slightly different manner, along the lines of quantum defect theory (QDT) [18].

We start with a pair of solutions of Eq. (3),  $f$  and  $g$ , that have regular,

$$f_{\nu}(x) = A_{\nu} x e^{-x^2/2} {}_1F_1(-\nu; \frac{3}{2}; x^2), \quad (5)$$

and irregular,

$$g_{\nu}(x) = B_{\nu} e^{-x^2/2} {}_1F_1(-\nu - \frac{1}{2}; \frac{1}{2}; x^2), \quad (6)$$

behavior at the origin, at any energy. Here  $\nu$  denotes a quantum number,  $\nu = \epsilon/2 - 3/4$ , while  $A_{\nu}$  and  $B_{\nu}$  are constants that will be determined later. In the following, our solutions are characterized by the subscript  $\nu$  instead of the subscript  $\epsilon$ . We calculate the asymptotic behavior of the two solutions using the known behavior of the confluent hypergeometric function,  ${}_1F_1$ ,

$${}_1F_1(a; b; x) \Big|_{x \rightarrow \infty} \rightarrow \frac{\Gamma(b)}{\Gamma(a)} x^{a-b} e^x + \cos(\pi a) \frac{\Gamma(b)}{\Gamma(b-a)} x^{-a}, \quad (7)$$

as well as the gamma reflection formula:

$$\Gamma(\nu) \Gamma(1 - \nu) = \frac{\pi}{\sin(\pi\nu)}. \quad (8)$$

For  $x \rightarrow \infty$ , we obtain

$$\begin{aligned} f_{\nu} &\rightarrow A_{\nu} \Gamma\left(\frac{3}{2}\right) \left( -x^{-2\nu-2} e^{x^2/2} \sin(\pi\nu) \frac{\Gamma(\nu+1)}{\pi} + x^{2\nu+1} e^{-x^2/2} \cos(\pi\nu) \frac{1}{\Gamma(\nu+\frac{3}{2})} \right), \\ g_{\nu} &\rightarrow B_{\nu} \Gamma\left(\frac{1}{2}\right) \left( -x^{-2\nu-2} e^{x^2/2} \cos(\pi\nu) \frac{\Gamma(\nu+\frac{3}{2})}{\pi} - x^{2\nu+1} e^{-x^2/2} \sin(\pi\nu) \frac{1}{\Gamma(\nu+1)} \right). \end{aligned}$$

Our goal is to recast these solutions in the “usual” QDT form [18] given by

$$f_\nu \rightarrow -C \left( D^{-1} e^{x^2/2} x^{-2\nu-2} \sin(\pi\nu) - D e^{-x^2/2} x^{2\nu+1} \cos(\pi\nu) \right), \quad (9)$$

$$g_\nu \rightarrow C \left( D^{-1} e^{x^2/2} x^{-2\nu-2} \cos(\pi\nu) - D e^{-x^2/2} x^{2\nu+1} \sin(\pi\nu) \right). \quad (10)$$

In addition, we want to normalize the functions  $f$  and  $g$  such that their Wronskian  $W[f_\nu, g_\nu]$  is  $2/\pi$ . These requirements can be fulfilled by defining  $A_\nu$  and  $B_\nu$  [Eqs. (5) and (6), respectively] appropriately, which leads to

$$f_\nu = \frac{2}{\sqrt{\pi}} \sqrt{\frac{\Gamma(\nu + \frac{3}{2})}{\Gamma(\nu + 1)}} x e^{-x^2/2} {}_1F_1(-\nu; \frac{3}{2}; x^2), \quad (11)$$

$$g_\nu = -\frac{1}{\sqrt{\pi}} \sqrt{\frac{\Gamma(\nu + 1)}{\Gamma(\nu + \frac{3}{2})}} e^{-x^2/2} {}_1F_1(-\nu - \frac{1}{2}; \frac{1}{2}; x^2). \quad (12)$$

Using these normalizations, the constants  $C$  and  $D$  [Eqs. (9) and (10)] become  $C = 1/\sqrt{\pi}$  and  $D = \sqrt{\pi}/\sqrt{\Gamma(\nu + 1)\Gamma(\nu + 3/2)}$ .

With these solutions for  $f$  and  $g$  in hand, we can proceed in the spirit of QDT by deriving a solution to the radial Schrödinger equation that accounts for an additional non-oscillator short-range potential. For distances beyond those where the short-range potential is non-negligible, the radial wave function  $u_\nu$  must assume the form

$$u_\nu = f_\nu \cos \pi\mu - g_\nu \sin \pi\mu. \quad (13)$$

Armed with the known asymptotic behavior of  $f$  and  $g$ , we can determine the asymptotic behavior of  $u$  and impose the requirement that  $u$  is finite at large  $x$  (i.e., the coefficient of the growing exponential is zero). This leads to the equality  $\sin \pi(\nu + \mu) = 0$ , which can be recast as a quantization condition

$$\epsilon = 2(n - \mu) + \frac{3}{2}, \quad (14)$$

where  $n = 0, 1, 2, \dots$ . The last step towards finding the energy levels  $\epsilon$  of our confined atom pair is to impose the boundary condition on the solution  $u$ , which is implied by the contact potential at the origin [Eq. (4)]. Using the fact that at small arguments  ${}_1F_1(a; b; x)$  approaches 1 [19], we obtain

$$\frac{u'(0)}{u(0)} = -\frac{f'(0) \cos \pi\mu}{g(0) \sin \pi\mu} = -\frac{a_{\text{ho}}}{a_{\text{sc}}}. \quad (15)$$

Upon inserting the explicit forms for  $f$  and  $g$  as given in Eqs. (11) and (12), we obtain the following equation for the quantum defect  $\mu$  (see also [17])

$$\tan \pi\mu = -\frac{a_{\text{sc}}}{a_{\text{ho}}} \frac{2\Gamma\left(\frac{\epsilon}{2} + \frac{3}{4}\right)}{\Gamma\left(\frac{\epsilon}{2} + \frac{1}{4}\right)}. \quad (16)$$

Equations (14) and (16) allow determination of the energy spectrum for any value of the scattering length  $a_{\text{sc}}$ . It can be shown that these equations are equivalent to the transcendental equation

$$\frac{2\Gamma\left(-\frac{\epsilon}{2} + \frac{3}{4}\right)}{\Gamma\left(-\frac{\epsilon}{2} + \frac{1}{4}\right)} = \frac{1}{a_{\text{sc}}/a_{\text{ho}}} \quad (17)$$

of Busch *et al.* [14]. The energy quantization conditions derived here for a zero-range pseudo potential using QDT also apply to a confined atom pair interacting through an arbitrary (i.e., non-contact) short-range potential, the only difference being that the quantum defect  $\mu$  has a different value. Regardless of the specific short-range potential, the corresponding eigenfunctions  $u_\nu$  are then given outside the potential range in terms of the hypergeometric U function [20, 14],

$$u_\nu(x) = N_\nu e^{-x^2/2} U\left(\frac{-(2\nu+1)}{2}, \frac{1}{2}, x^2\right),$$

where  $N_\nu$  is a normalization constant.

### 3. Two atoms near a Feshbach Resonance. Overlap matrix elements

To apply our formalism derived above to two-atom states that lie energetically near a Feshbach resonance, we rewrite our scattering length  $a_{\text{sc}}$  as a function of the magnetic field strength  $B$

$$a_{\text{sc}}(B) = a_{\text{bg}} \left(1 - \frac{\Delta}{B - B_0}\right).$$

Here,  $a_{\text{bg}}$  denotes the scattering length far from the resonance,  $B_0$  denotes the resonance position, while  $\Delta$  is a parameter related to the width of the resonance. In our numerical calculations (see Sec. 5), we choose parameter values according to recent multichannel calculations [8] of the Feshbach resonance in  $^{85}\text{Rb}$ :  $B_0 = 154.9$  G,  $\Delta = 9.907$  G, and  $a_{\text{bg}} = -450$  a.u. Note that a similar model was employed in Ref. [16] for the case of a Feshbach resonance in  $^{23}\text{Na}$ . While that study additionally incorporated an energy dependence of the scattering length, the energy dependence of the scattering amplitude in the present study is comparatively weak over the energy range considered that we choose to neglect it.

Our goal is to describe our two-atom system when it is subjected to time-dependent magnetic field ramps  $B(t)$ , like the ones used in the experiments of [1]. To approximate the experimental  $B(t)$ , we assume a piecewise constant  $B(t)$  as indicated in Fig. 3. In our approach the assumption of an instantaneous variation of  $B(t)$  amounts to the use of the sudden approximation. In this approximation, the wavefunction of the atom pair is initially unaffected by the instantaneous change of  $B(t)$ . Let the magnetic field strength before (after) the instantaneous change be  $B_1$  ( $B_2$ ). It is then convenient to write the time-dependent superposition state  $\Psi$  at field strength  $B_1$  in terms of the eigenfunctions  $\{\phi_{\nu_1}\}_{\nu_1=0,\infty}$  (with corresponding eigenvalues  $\{\epsilon_{\nu_1}\}_{\nu_1=0,\infty}$ ), and that at field strength  $B_2$  in terms of the eigenfunctions  $\{\phi_{\nu_2}\}_{\nu_2=0,\infty}$  (with corresponding eigenvalues  $\{\epsilon_{\nu_2}\}_{\nu_2=0,\infty}$ ),

$$\Psi(B_j, t) = \sum_{\nu_j} a_{\nu_j}^{(j)}(t) \phi_{\nu_j}, \quad j = 1, 2. \quad (18)$$

The “new” expansion coefficients  $a_{\nu_2}^{(2)}$  can be expressed through the “old” expansion coefficients,

$$a_{\nu_2}^{(2)} = \sum_{\nu_1} O_{\nu_2, \nu_1} a_{\nu_1}^{(1)},$$

where  $O_{\nu_2, \nu_1}$  denotes the overlap matrix between the eigenfunctions corresponding to  $B_1$  and  $B_2$ , respectively,

$$O_{\nu_2, \nu_1} = \langle \phi_{\nu_2} | \phi_{\nu_1} \rangle. \quad (19)$$

The following derivation shows how the eigenstate transformation projections  $O_{\nu_2, \nu_1}$  can be determined analytically. Let  $u_{\nu_{1,2}}$  be the reduced radial wavefunctions corresponding to  $\phi_{\nu_{1,2}}$ . If we multiply the equation for  $u_{\nu_1}$  by  $u_{\nu_2}$  and that for  $u_{\nu_2}$  by  $u_{\nu_1}$ , subtract the resulting equations and integrate the result from 0 to  $\infty$ , an integration by parts gives

$$(\epsilon_{\nu_1} - \epsilon_{\nu_2}) \int_0^\infty u_{\nu_1}(x) u_{\nu_2}(x) dx = W [u_{\nu_1}, u_{\nu_2}]_{x=0}. \quad (20)$$

Here,  $W [u_{\nu_1}, u_{\nu_2}]_{x=0}$  denotes the Wronskian of  $u_{\nu_1}$  and  $u_{\nu_2}$  evaluated at the origin. The above formula allows the determination of both the normalization constant  $N_\nu$  [Eq. (2)] and the overlap matrix element  $O_{\nu_2, \nu_1}$  [Eq. (19)],

$$O_{\nu_2, \nu_1} = N_{\nu_1} N_{\nu_2} \left[ 2 \cos(\pi \nu_1) \Gamma\left(\frac{3}{2} + \nu_1\right) \Gamma(1 + \nu_2) \sin(\pi \nu_2) \right. \\ \left. - 2 \cos(\pi \nu_2) \Gamma(1 + \nu_1) \Gamma\left(\frac{3}{2} + \nu_2\right) \sin(\pi \nu_1) \right] / [4 \pi (\nu_2 - \nu_1)] \quad (21)$$

and

$$N_\nu = \left\{ \Gamma(1 + \nu) \Gamma\left(\frac{3}{2} + \nu\right) \left[ 2\pi + \left( \psi(\nu) - \psi\left(\frac{1}{2} + \nu\right) \right) \sin(2\pi\nu) \right] \right\}^{-1/2}, \quad (22)$$

where  $\psi$  denotes the digamma function [19]. The overlap matrix elements  $O_{\nu_2, \nu_1}$  are expressed in terms of the  $\nu$  quantum numbers, which, in turn, are directly linked to the energy eigenvalues  $\epsilon$  through  $\epsilon = 2\nu + 3/2$ . Figure 1 shows examples of the dependence of the overlap matrix elements on the non-integer quantum numbers  $\nu_1$  and  $\nu_2$ . While the overlap matrix elements oscillate rapidly with  $\Delta\nu$  ( $\Delta\nu = \nu_2 - \nu_1$ ), our analytical formula for the overlap matrix elements results in stable numerical calculations (see Sec. 5).

#### 4. Description of many-body effects through a frequency rescaling

The simple model described in the previous section allows us to describe the states of a trapped atom pair that undergoes sudden changes of the interatomic interaction, here parametrized accurately through a magnetic field-dependent scattering length. Our goal is now to apply our two-atom model to interpret an ensemble of  $N$  atoms ( $N \gg 2$ ). Without constructing a rigorous many-body approach like, e.g., the ones based on the field theory formalism, we will attempt to account for many-body effects by using our two-particle model with a rescaled frequency. The idea suggested by Cornell [21] is to capitalize on the importance of the diluteness parameter  $N(a_{\text{sc}}/a_{\text{ho}})^3$ , which in more rigorous many-body models of degenerate Bose gases plays a key role in determining the behavior of the system. Instead of modeling an  $N$ -atom system we will model a two-body system that has the same diluteness parameter as the experimentally studied  $N$  atom system.

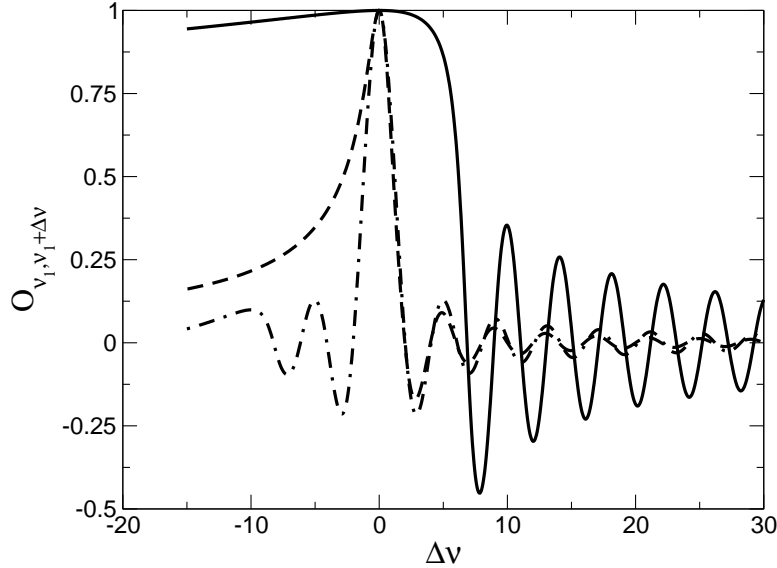


**Figure 1.** Dependence of the overlap matrix element  $O_{\nu_2, \nu_1}$  between two eigenfunctions corresponding to quantum numbers  $\nu_1$  and  $\nu_2 = \nu_1 + \Delta\nu$  on the quantum number difference,  $\Delta\nu$ , for three values of  $\nu_1$ :  $\nu_1 = -5$  (solid line),  $\nu_1 = 1.5$  (dashed line), and  $\nu_1 = 10$  (dashed-dotted line). Note that the solid line in this figure represents the projections of the molecular state onto the other trapped atoms states.

To motivate that our two-body description can, at least to a crude level of approximation, account for many-body physics we calculate the overlap integral for one particular case. We consider the overlap integral between a two-body state located very far from the resonance centered at  $B_0$ ,  $u_{\text{ho}}(r)$ , with that corresponding to a value of  $B$  close to  $B_0$ ,  $u_M(r)$ .  $u_{\text{ho}}$  refers to the trap ground state, which we approximate through a state describing two independent atoms with zero scattering length,

$$u_{\text{ho}}(x) \approx \frac{2}{\pi^{1/4}} x e^{-x^2/2} \quad (23)$$

$u_M(r)$  denotes a molecular state (i.e., the state that remains bound even in the absence of the confining potential). Neglecting the influence of the confining potential we assume the wavefunction of this state to be:

$$u_M(r) \approx \sqrt{2\kappa} e^{-\kappa r}, \quad (24)$$

where  $\kappa = 1/a_{\text{sc}}$ . We estimate the overlap integral of these two states, by assuming that the exponential in  $u_{\text{ho}}$  is approximately 1 over the range relevant for the evaluation of the integral. This approximation yields

$$\langle u_M | u_{\text{ho}} \rangle \approx \left( \frac{2a_{\text{sc}}}{a_{\text{ho}}} \right)^{3/2} \pi^{-1/4}. \quad (25)$$

The absolute value of this overlap matrix element gives the probability  $p$  that the initially “unbound” atom pair ends up in the molecular state as the  $B$  field is tuned close to

resonance,

$$p = \frac{8}{\sqrt{\pi}} \left( \frac{a_{\text{sc}}}{a_{\text{ho}}} \right)^3. \quad (26)$$

For small  $p$  ( $p \ll 1/N$ ), we can extend our two-body treatment to model an ensemble of  $N$  atoms. As the  $B$  field is tuned to resonance, *each atom pair* in the ensemble has the probability  $p$  to form a molecular bound state. Using this simple picture, the calculation of the fraction of atoms that transform into molecules,  $f_{\text{atoms} \rightarrow \text{molecules}}$ , due to the magnetic field ramp amounts to a simple counting of atom pairs,

$$f_{\text{atoms} \rightarrow \text{molecules}} = \frac{2}{N} \frac{N(N-1)}{2} p \approx Np = \frac{8}{\sqrt{\pi}} \frac{a_{\text{sc}}^3 N}{a_{\text{ho}}^3}. \quad (27)$$

Within our estimate, the fraction of atoms transformed to molecules depends on the diluteness parameter  $N a_{\text{sc}}^3 / a_{\text{ho}}^3$ . This back-of-the-envelope estimate, although not a rigorous proof, provides a somewhat quantitative motivation for the frequency rescaling introduced above.

Since the diluteness parameter scales as  $\omega^{3/2}$ , the new angular frequency  $\omega'$  is given through  $\omega' = \omega N^{2/3}$ . This relation defines a new value for the associated harmonic oscillator length  $a_{\text{ho}}' = a_{\text{ho}} / N^{1/3}$ . The experiment [1] uses an inhomogeneous trap that has a geometric mean of  $\omega = 2\pi 10.9$  Hz, and also involves approximately  $N = 17100$  atoms. With these parameters, the above rescaling yields  $\omega' = 2\pi 7.23$  kHz. Figure 2 shows the eigenvalues of two  $^{85}\text{Rb}$  atoms confined by a harmonic potential with angular frequency  $\omega'$  as a function of the magnetic field strength  $B$  in the vicinity of the Feshbach resonance described through the parameters given in Sec. 3. Notice that the sequence of avoided crossings of energy levels associated with the Feshbach resonance becomes smeared out at this high frequency. We group the two-body states into three groups (see Fig. 2): the molecular state, the trap ground state, and the excited states of the trap. To connect our two-body study to the  $N$ -body systems studied experimentally, we make the following correspondence between the two-atom states and the many body states. The molecular state of two atoms is in the ground state of the center-of-mass motion, and accordingly we associate this population with translationally cool (condensed) molecules in the  $N$ -atom system. At fields above the resonance, the lowest *positive* energy state (which we refer to as the trap ground state) corresponds to condensate atoms. Finally, the higher trap excited states correspond to non-condensed atoms, i.e., the experimentally observed “jets of hot atoms” [1]. In the next section, we interpret the occupation probability of the two-atom states as the fraction of atoms ending up in the corresponding many body states.

## 5. Numerical Results

We now use the above description to simulate the experiment of Donley *et al.* [1]. This experiment consists of applying two magnetic field pulses, separated by a time interval of variable length (denoted by  $t_{\text{evolve}}$  in Fig. 3), to a condensed sample of  $^{85}\text{Rb}$  atoms. The two pulses of lengths  $t_1$  and  $t_2$ , respectively, ramp the magnetic field to

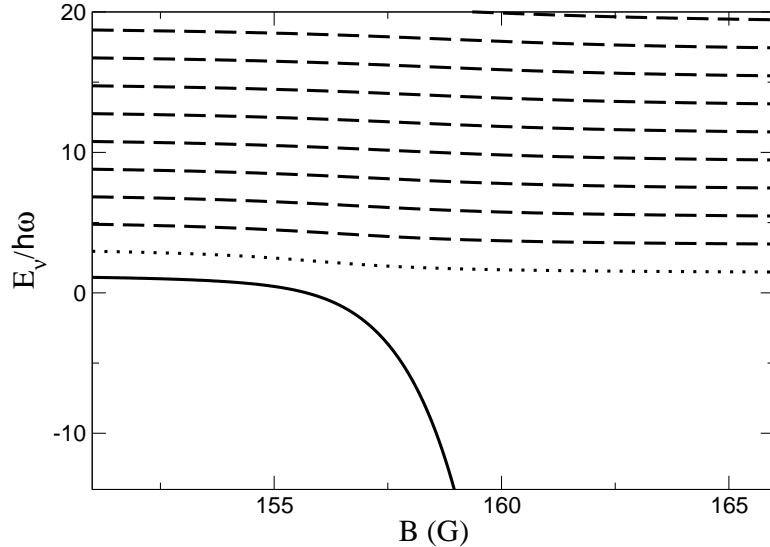


**Figure 2.** Energy eigenvalues for two  $^{85}\text{Rb}$  atoms for a rescaled frequency  $\omega' = 2\pi 7.23$  kHz (corresponding to  $N = 17100$ ) near a Feshbach resonance centered at  $B_0 = 154.9$  G with  $a_{\text{bg}} = -450$  a.u. and  $\Delta = 9.907$  G. We distinguish three groups of states: the molecular state (solid line), the trap ground state (dotted line), and the trap excited states (dashed lines).

$B_m$ , a value close to the Feshbach resonance, which couples the atomic and molecular states of the sample. After the application of these magnetic pulses, three distinct components are identified experimentally: a remaining sample of condensed atoms, a hot burst of atoms, and a “missing” component which is not detected under the current experimental conditions. At least two theoretical approaches [8, 9], both involving a field theory formalism, identified this third component (i.e., the missing component) as a molecular condensate, however, other interpretations exist. The size of the three components oscillates as a function of the evolve time  $t_{\text{evolve}}$  with a frequency that corresponds to the energy of a weakly bound, vibrationally excited state, of the  $^{85}\text{Rb}_2$  dimer.

We model the experimental situation using the sudden approximation to describe the sharp rises and drops of the magnetic field. At time  $t = 0$  in Fig. 3, our initial state is chosen to be the trap ground state corresponding to the initial value of the magnetic field,  $B_i$ . This initial state is then propagated in time. During the time period where the magnetic field is unchanged,  $B(t) = B_i$ , the time propagation simply modulates the phase of the initial state. After the magnetic field changes to the value  $B(t) = B_m$ , the system is projected onto the new eigenstates at that field. We then propagate the quantum amplitudes of the two-atom energy eigenstates. At the end of the double pulse, when the magnetic field becomes  $B_f$ , our final state is expanded in the  $\phi_\nu$  states corresponding to the final value of the magnetic field,  $B_f$ . Using the correspondence

**Table 1.** Comparison of the relevant values of the magnetic field,  $B$  (in Gauss) and of the corresponding scattering length,  $a_{sc}$  (in atomic units) for the pulses used in the present calculation and the one presented by Donley *et al.* [1].

	Present calculation		Experiment of Ref. [1]	
	$B$ (G)	$a_{sc}$ (a.u.)	$B$ (G)	$a_{sc}$ (a.u.)
$B_i$	163.5	68.4	162	177.9
$B_m$	157.9	1036	155.5	6980
$B_{evolve}$	159.77	465.4	159.84	452.46
$B_f$	163	100.4	161.75	200.8

between two-body and many-body states discussed in the previous section, we then relate the final population probabilities to the Donley *et al.* experiment. In taking the absolute square of this final quantum amplitude for each distinguishable final state, cross terms arise that exhibit quantum beats, the most prominent of which is between the molecular state and the atomic trap ground state (condensate).

The parameters entering our simulations are the rescaled frequency  $\omega'$ , the four magnetic field values  $B_i$ ,  $B_{evolve}$ ,  $B_m$  and  $B_f$ , as well as the three time periods  $t_1$ ,  $t_{evolve}$  and  $t_2$ . Our particular simulation values are given in the caption of Fig. 3. We have adjusted the fields  $B_i$ ,  $B_m$ , and  $B_f$  to see whether a small modification can give good agreement with the measured populations. In fact, we found good agreement as shown in Fig. 4 (compared to Fig. 6 of Ref. [1]) provided those three fields differ from the experimental values by 1-2 G. The Feshbach resonance parameters used in these calculations to determine the scattering lengths at those fields were given in Sec. 3. Since  $B_{evolve}$  controls the molecular binding energy, it therefore determines the oscillation frequency of the individual many-body components. We choose a value for  $B_{evolve}$  (159.77 G) very close to that of the experiment (159.84 G). Our changes of the magnetic fields that characterize the pulses produces differences in the scattering length at those fields. These differences are summarized in Table 1. Most notable is the difference of the scattering length at  $B = B_m$  which is considerably larger in the experiment (approximately 6 times according to our estimate) than the value of  $a_{sc}$  used in our calculations.

Figure 4 shows the results of our time-dependent two-atom calculation for a scaled frequency  $\omega'$  that gives a density comparable to an initial condensate with  $N = 17100$  atoms and an unscaled trapping frequency  $\omega = 2\pi 10.9$  Hz. This figure can be directly compared with Fig. 6 of Ref. [1]. Inspection of these two figures shows reasonable agreement in the average values and the oscillation amplitudes for the three components. The largest qualitative disagreement between our results and those in Fig. 6 of Donley *et al.* regards the phase shifts of the oscillations of the different populations which are much smaller in our results. Note that our rescaled frequency yields  $\hbar\omega'/k_B \approx 350$  nK, which implies that the first excited level above the trap ground state is a few times more

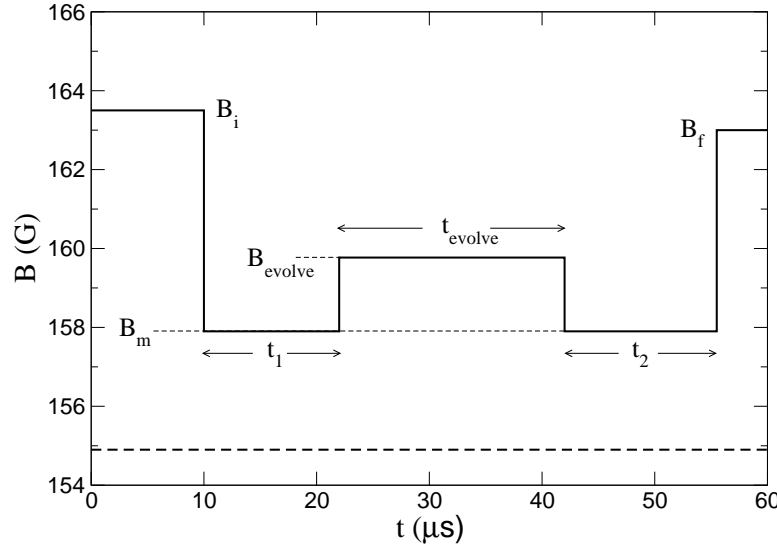


**Figure 3.** Magnetic field  $B$  as function of time  $t$  in our modeling of the experiments of Donley *et al.*. The thick dashed line represents the position of the Feshbach resonance,  $B_0 = 154.9\text{G}$ . The abrupt variations of the magnetic field reflect our use of the sudden approximation. The parameters of the pulse are:  $B_i = 163.5\text{ G}$ ,  $B_m = 157.9\text{ G}$ ,  $B_{\text{evolve}} = 159.77\text{ G}$ ,  $B_f = 163\text{ G}$ , and  $t_1 = 12\text{ }\mu\text{s}$ ,  $t_2 = 13.6\text{ }\mu\text{s}$ .

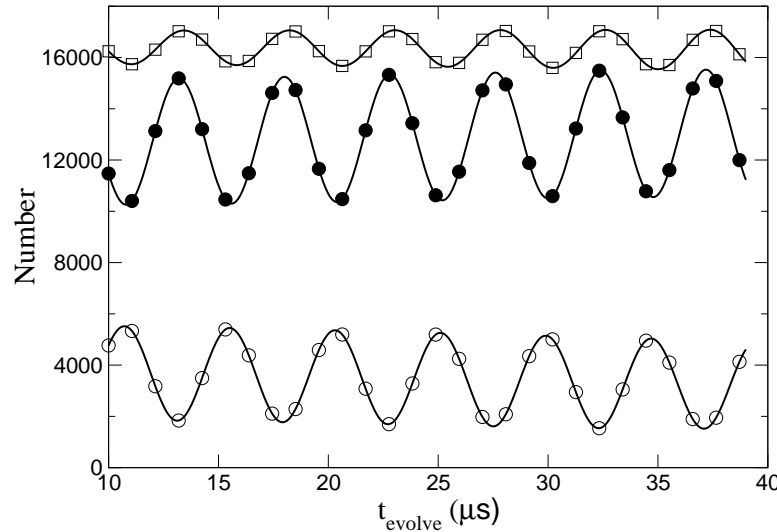


**Figure 4.** Population of the ground trap state (filled circles) and of the excited trap states (open circles) at the end of the magnetic field pulse shown in Fig. 3. The sum of the two populations is plotted with squares and allows determination of the number of atoms that made the transition to molecules by subtraction from the total number of atoms ( $N = 17100$ ).

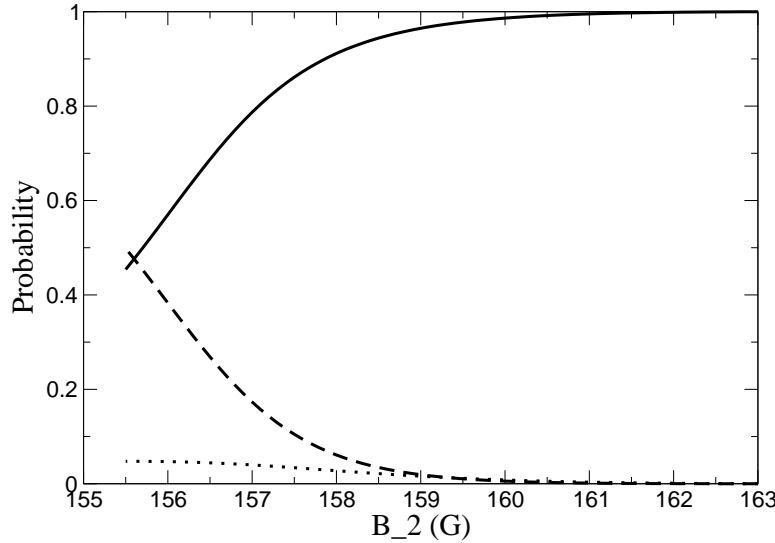


**Figure 5.** Transition probability after a single, sudden change of the magnetic field from  $B_1 = 163.5$  G to  $B_2$ , plotted as a function of the value of  $B_2$ . The initial state is the trap ground state (atomic BEC) at  $B_1$ . The final states at  $B_2$  are: the trap ground state (solid line), the molecular state (dashed line), and the excited states of the trap (dotted line).

energetic than the observed energy (150 nK) of the burst atoms. The rescaling used in our model thus allows a reasonable prediction of the number of the hot atoms, but it precludes an accurate prediction of their energy.

As mentioned above, the relative phases of the condensate, molecule, and hot-atom oscillations are not described as accurately in the present two-atom treatment as they are in the field theoretic descriptions. [8, 9] The two-atom model does show a nontrivial phase difference among the three components, at other values of the magnetic field ramp parameters, but it is beyond the scope of this paper to address the systematics of these phase differences.

Fig. 5 shows the probability for an atom pair to end up in one of the three groups of states after only one magnetic field ramp (assuming that we start in the trap ground state corresponding to  $B_1 = 163.5$  G). Most notable is the dramatic increase of the molecular state probability as  $B_2$  gets closer to the resonance. This shows the reason why we needed a comparatively higher value of  $B_m$  in order to achieve agreement with the experiment. When the pulses in our simulation adopted values of  $B_m$  closer to the resonance position, (i.e., closer to the experimental situation), it resulted in a larger depletion of the BEC state and also a larger amplitude of the oscillations of the three components compared to the experiment. Figure 6 shows the evolution of the population during only one pulse (with  $t_{\text{evolve}} = 20 \mu\text{s}$ ) as a function of time. According to our calculations, the molecular eigenstate and the excited states (i.e., the non-condensed atoms) are populated with

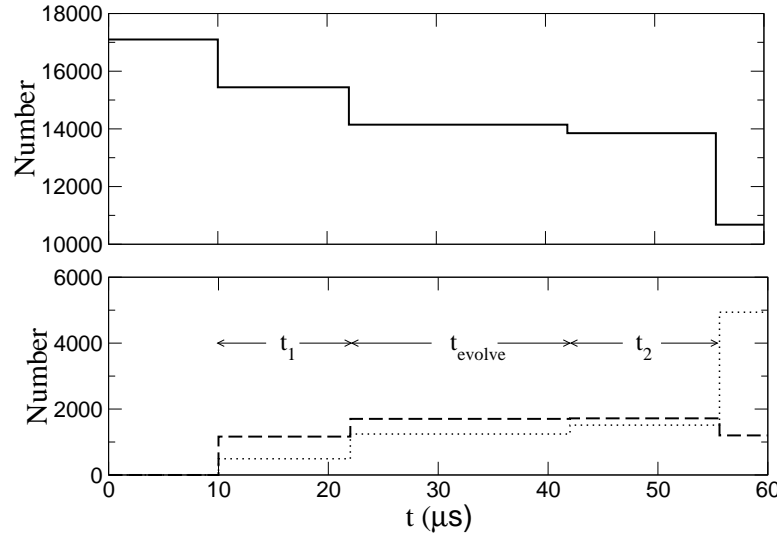


**Figure 6.** Evolution of population of the three types of states as a function of time during one magnetic field double-pulse (with  $t_{\text{evolve}} = 20 \mu\text{s}$ , same as the one plotted in Fig. 3). The top panel depicts the trap ground state (condensate) population while the bottom panel shows the molecular (dashed line) and excited trap states (dotted line) populations.

roughly equal populations when the magnetic field is ramped the first time, at the beginning of the first pulse. Those same two components retain a comparable population until the last ramp of the pulse, when the population of the excited states becomes considerably larger.

The significant population we observe for the molecular state during  $t_{\text{evolve}}$  supports our interpretation of the quantum beats seen in the end-of-pulse populations. These beats are the result of the interference of quantum paths that go through the intermediate molecular state with those that go through the intermediate ground or excited trap states. (The difference between the latter is too small to show up on the time scales considered here.) The predictions of this two-atom model, concerning the intermediate time populations of the molecular and hot components, are consistent with the comments of Braaten *et al.*, [10] which point out the difficulty of interpreting the intermediate populations shown in Ref. [8]. Interpretation of the results of Kokkelmans and Holland [8] is complicated by the fact that their two-body representation does not consist of eigenfunctions of the molecular Hamiltonian. Accordingly, their "molecular state" is not actually the two-body molecular eigenstate, except at magnetic fields well above 160 G. In problems with a linear Schrödinger equation, a simple basis change could always be carried out, to re-express the physics in an eigenrepresentation. Here, however, the nonlinearity of the coupled equations makes this transformation far more complicated to carry out. At the same time, as Braaten *et al.* [10] comment, the success of the final calculations in reproducing the experimental observations with no

adjustable parameters is immediately apparent and convincing that the right two-body physics has been incorporated into the formulation. We mainly recommend caution in interpreting the meaning of the “molecular state” in the Kokkelmans and Holland formulation, except at high magnetic fields where it approximately coincides with a two-body eigenstate.

The two-atom model disagrees with a specific qualitative prediction of Mackie *et al.* [11]. Whereas in our model the “hot” atoms at the end of the pulse can be created through any of the three intermediate states (i.e, molecules, condensed atoms or non-condensed atoms), in the model of Ref. [11] the “hot” atoms are solely the results of the “rogue dissociation” of intermediate molecular states. Our approach suggests that a substantial fraction of the final hot atoms are not produced by rogue dissociation. In fact, it is predominantly the pathway *condensate*  $\rightarrow$  *hot atoms*, which is apparently neglected by Ref. [11]. This may in fact be the additional loss mechanism that is cited as being “missing” in Ref. [11].

## 6. Conclusions

We have investigated the results given by a simple model of the dynamics of two trapped atoms near a Feshbach resonance. Our model accounts for the interaction between the two atoms using a zero range potential and it also includes the confinement of the atoms by an external harmonic trap. This model can be used to make predictions regarding BEC driven with the help of magnetic fields near a Feshbach resonance, if a rescaled frequency is used to achieve a density comparable to the density of the many-atom condensates studied experimentally. A correspondence can be drawn between the three components observed in the recent field-ramp experiments and three groups of two-body states in our model. The experimentally-observed burst of hot atoms appears in this model as atom pairs excited to states energetically higher than the trap ground state level. The two-atom model is able to predict the populations of these three states, in fair agreement with the experimental observations. Accordingly this may provide a useful alternative view of the physics of coherent atom-molecule coupling in a condensate. The success of a two-body description may initially seem surprising, because the dominant physical processes occurring in condensate experiments near a Feshbach resonance are normally viewed as being inherently many-body in nature. Nevertheless, the present study suggests that a two-body picture is sufficiently realistic to be used for simple estimates at a qualitative or semiquantitative level.

## Acknowledgments

We thank E. Cornell for helpful suggestions and encouragement. We also thank N. Claussen, J. Dunn, M. Holland, and C. Wieman for informative discussions. This work was supported by NSF.

## References

- [1] Donley E A, Claussen N R, Thompson S T and Wieman C E 2002 *Nature* **417** 529
- [2] Zoller P 2002 *Nature* **417** 493
- [3] Heinzen D J, Wynar R, Drummond P D and Kheruntsyan K V 2000 *Phys. Rev. Lett.* **84** 5029
- [4] Inouye S, Andrews M R, Stenger J, Miesner H -J, Stamper-Kurn D M and Ketterle W 1998 *Nature* **392** 151
- [5] Cornish S L, Claussen N R, Roberts J L, Cornell E A and Wieman C E 2000 *Phys. Rev. Lett.* **85** 1795
- [6] Timmermans E, Tommasini P, Côté R, Hussein M and Kerman A 1999 *Phys. Rev. Lett.* **83** 2691
- [7] Claussen N R, Donley E A, Thompson S T and Wieman C E 2002 *Phys. Rev. Lett.* **89** 010401
- [8] Kokkelmans S J J M F and Holland M J 2002 *Phys. Rev. Lett.* **89** 180401
- [9] Köhler T, Gasenzer T and Burnett K 2003 *PR A* **67** 013601
- [10] Braaten E, Hammer H W, Kusunoki M 2003 Comment on “Ramsey Fringes in a Bose-Einstein Condensate between Atoms and Molecules” *Preprint cond-mat/0301489*
- [11] Mackie M, Suominen K -A and Javanainen J 2002 *Phys. Rev. Lett.* **89** 18403
- [12] Duine R A and Stoof H T C 2003 *cond-mat/0302304*
- [13] Andrä H J 1970 *Phys. Rev. Lett.* **25** 325
- [14] Busch T, Englert B -G, Rzäżewski K and Wilkens M 1997 *Found. Phys.* **28** 549
- [15] Tiesinga E, Williams C J, Mies F H and Julienne P S 2000 *PR A* **61** 063416
- [16] Bolda E L, Tiesinga E and Julienne P S 2002 *Phys. Rev. A* **66** 013403
- [17] Blume D and Greene C H 2002 *Phys. Rev. A* **65** 043613
- [18] Greene C, Fano U and Strinati G 1979 *Phys. Rev. A* **19** 1485
- [19] Abramowitz M and Stegun I A 1970 *Handbook of Mathematical Functions* (New York: Dover Publications, Inc.) p. 504
- [20] See eq. 13.1.3 of Ref. [19]
- [21] Cornell E A *private communication*